Noname manuscript No.
(will be inserted by the editor)

Knowledge Management in Image-based Analysis of Blood Vessel Structures

Iván Macía · Manuel Graña · Celine Paloc

the date of receipt and acceptance should be inserted later

Abstract We have detected the lack of a widely accepted knowledge representation model in the area of Blood Vessel analysis. We find that such a tool is needed for the future development of the field and our own research efforts. It will allow easy reuse of software pieces through appropriate abstractions, facilitating the development of innovative methods, procedures and applications. After the identification of the key representation elements and operations, we propose a Vessel Knowledge Representation (VKR) model that would fill this gap. We give insights on its implementation based on standard Object Oriented Programming (OOP) tools and paradigms. The VKR would easily integrate with existing medical imaging and visualization software platforms, such as ITK and VTK.

Keywords Vessel Analysis · Knowledge Representation · Medical Image

1 Introduction

Vascular-related diseases are among the most important public health problems nowadays. Heart and cerebrovascular diseases are respectively the first and third cause of death in 2006 in the U.S.A [34]. Malignant tumors are the second cause of death, and their growth is directly associated with vessel recruitment and angiogenesis [35]. Besides, vascular diseases are one of the principal causes of death and disability in people with diabetes [21]. These facts are enough justification for the research efforts providing a better understanding of the structure of the vascular system and related processes and diseases, and leading to any improvement of diagnostic and intervention procedures.

Iván Macía, Celine Paloc
Vicomtech, Visual Communications Technologies Centre,
http://www.vicomtech.org
E-mail: imacia@vicomtech.org

M. Graña
Grupo de Inteligencia Computacional, UPV/EHU,
http://www.ehu.es/ccwtinco

The vessel structure of the blood circulatory system is one of the most complex structures of the body. Blood vessel anatomy has been studied from castings and in-vivo examinations in order to build models that provide valuable insight into the normal and variant circulatory anatomy and that helps to understand the causes, evolution and outcome of several vascular-related diseases. However, many answers to simple questions about vascular morphology and angiogenesis remain open[85].

Recent advances on medical imaging provide high resolution images of the vessel structures, so that the generation of accurate patient-specific geometric *in-vivo* vessel models [6] and related quantitative measurements has become feasible. This has resulted in a wide range of new applications for computer-assisted diagnostic, intervention and follow-up of vascular-related diseases. Image-based vessel analysis provides valuable information for planning and navigation during interventional procedures, both to avoid damaging vital structures and to use vessels as anatomical landmarks for orientation and localization of structures of interest. Moreover, comprehensive image-based vascular analysis has opened new horizons in the discovery and understanding of the vascular structure and underlying processes, such as angiogenesis and blood circulation, that may help to understand the evolution of diseases in which vascular structures play an important role [9] [86]

The diversity of medical and biological applications and the availability of huge amounts of high-quality information for vessel analysis has raised the problem of vascular knowledge representation in its full multi-faceted complexity . The purpose of this paper is to discuss appropriate knowledge representation and manipulation tools for vessel structures which could serve as a common ground for the development of compatible and reusable systems. We frame this study in the diversity of applications found in the literature, and in our actual research experience [57,50,61,60,58,62,59]. We contribute a *Vessel Knowledge Representation* (VKR) model that, due to its efficiency and versatility, may be used for a wide variety of image-based vessel extraction schemes and vessel analysis applications. This model aims to fill an information management gap that we have detected in the literature dealing with vessel structures computerized extraction and analysis of vascular structures.

We have in mind two objectives when proposing the *Vessel Knowledge Representation* (VKR) *Model*:

1. to ease the definition of new algorithms, providing a kind of road map of tools and applications.
2. to allow the easy reuse of previously generated pieces of software. The visualization of image processing as a kind of pipeline, allows the visualization of software reutilization as building blocks in this pipeline. This approach is common to some other medical imaging processes, like brain mapping.

The structure of the paper is as follows. In Section 2 we provide a review of the topics of interest related to the definition of the VKR model: knowledge on vascular morphology, vessel-related diseases, angiographic diagnosis, vessel extraction and analysis techniques from these images and corresponding applications. As a corolary, in Section 3 we describe the requirements for a Vessel Knowledge Representation model, which is described in Section 4. Finally we provide some implementation details (Section 5) and some final conclusions (Section 6).

2 Background Facts and Motivations

Here we review some background ideas about Vascular Morphology that influence the definition of an abstract vessel representation. Some facts of vascular related diseases serve as an introduction for the main applications in the field of modelling and visualization of vessel structures. Next, we provide an overview of the angiographic modalities for image-based diagnostic of vascular-related diseases, as well as the applications and vessel information which is considered relevant for diagnosis in the clinical practice. We will comment on the current computational techniques for vessel information extraction from the angiographic images. Finally we discuss the need for a knowledge representation model in this area.

2.1 Vascular Morphology

The efficient distribution and collection of nutrients requires a branching tree structure for the blood vessels, except at the level of the capillaries. Vascular networks are asymmetric tree structures, in which each parent branch, with Diameter D_1, is bifurcated (except in very rare cases) into two branches with smaller diameters (D_2 and D_3). The tree may be also locally unbalanced regarding the diameters of child branches ($D_2 \neq D_3$) and the number of bifurcations along each path from the root to the leaves of the each subtree [42]. Geometric models for the description of vessel bifurcations were first proposed by Murray [67,90] and later by Oka and Nakai [71] specifying relationships between vessel widths and angles based on physiological observations.

Recent studies [43,110] have discovered that the construction of the vascular trees obeys a set of scaling laws which minimize both, the energy cost of fluid transportation, which decreases as the diameters increase, and the energy cost of construction and maintenance of the vessel structure, which increases with larger diameters. These scaling laws are morphometric relationships between the arterial volume, cumulative length, and diameter of a branch and its distal subtree. In particular, it can be seen that, in order to minimize the power needed to maintain the blood circulation operation over the network, the diameter relationship between a parent branch and its two child branches is:

$$D_1^k = D_2^k + D_3^k, \tag{1}$$

with average values of k typically between 2 and 3.

With respect to the vessel sections, in a simplistic approach the vessel sections can be assumed to be circular but, in fact, most of the times it has some smooth irregular round shape. The thickness of the vessel wall is non-negligible, but most imaging modalities only depict the vessel *lumen*, which is the space where the blood flows. Few imaging modalities, such as Intravascular Ultrasound (IVUS), can image the vessel wall.

In order to estimate the complexity and branching frequency of the human vascular trees [22,93,36,38,37,39], several studies used and adapted the *Strahler order* of branching complexity [95], defined originally for hidrology studies but applicable to all branching, tree-like structures. The original Strahler ordering system follows these rules:

- The smallest branches are defined as of order 1.

- When two vessels of the same order join into a confluent vessel, the order of the confluent vessel is increased by 1.
- When a vessel of order n joins a vessel of order lower than n, the order of the confluent vessel remains n.

However, the use of the original order as defined by Strahler encountered the problem of diameter overlapping among vessels of consecutive orders when applied to vessel morphometry of very large trees. In order to take into account the vessel radius, the *Diameter-defined Strahler Ordering System* was defined [44]. This ordering system includes a new rule:

- When a vessel of order n meets another vessel of order $\leq n$, the confluent vessel is assigned order $n+1$ only if its diameter exceeds that of the lower order vessel by a certain amount, which is determined by the statistical distribution of the diameters of each order. Typically, assuming statistical normality, the threshold will be the mean plus and minus one standard deviation.

In practice, this calculation is iterative, since the diameter distribution has to be recalculated when the order is assigned. Applied to haemodynamic studies, this enhanced ordering system provides a reasonable and systematic way to handle main arteries that vary considerably in diameter along their length, such as the main pulmonary artery.

In order to represent the connectivity of asymmetric branches and to distinguish serial and parallel branches of the same order, three new concepts where introduced in [44]: *Vessel Segment*, *Vessel Element* and *Connectivity Matrix*. A *Vessel Segment*, corresponding to a branch, is the portion of vessel between two bifurcations. A *Vessel Element* is defined as a set of serially connected segments of same order. Statistical data of diameters and lengths are obtained for segments and elements. Haemodynamic flow circuits are composed of vessel elements. Ratios of segment/element can also be calculated for each order. The *Connectivity Matrix* is an upper triangular matrix, in which each element $C(m,n)$ is the ratio of the total number of elements of order m whose parents are elements of order n divided by the total number of elements of order n. In a morphometric study of the human lung vasculature casts [39] it was found that, in pulmonary arterial and venous trees, the relationship between the order of a branch [44] and its diameter follows closely a logarithmic scale. They found a maximal order of 15 for both arterial and venous trees of the human lung.

2.2 Vascular-related Diseases

There are two main types of vascular accidents which occur with death consequences in about 5% of the population over 65 years-old: haemorrages and embolysms. Haemorrages can be produced by vessel ruptures due to aneurysms. An *aneurysm* is a local growth of the vessel diameter due to weakening of the vessel wall that suffers increased local elasticity. Aneurysms occur most commonly in arteries at the base of the brain (circle of Willis) and in the thoracic and abdominal aorta. Embolysms and thrombosis are obturations of the vessels as a consequence of a progressive abnormal local reduction or the vessel diameter or *stenosis* (pl. stenoses). There are several causes or conditions that lead to stenosis such as atherosclerosis, birth defects, diabetes, infection, inflammation or ischemia among others. Atherosclerosis is a condition in which the arterial wall thickens, due to the accumulation of a mixture of substances such as

calcium, cholesterol fibrin and macrophage blood cells, which causes stenosis or occlusion of the vessel or aneurysms due to excessive compensation by enlargement of the vessel. The possibility of performing early diagnoses of aneurysms, stenoses or other vascular accidents may avoid further complications and thus, will decrease the morbidity and mortality associated to vascular-related diseases. There exists evidence [7] that regions of the vessel wall exposed to disturbed flow, such as at bifurcations and regions of high curvature, are prone to the initiation and development of atherosclerosis. Identification of such regions by geometrical analysis may provide further insight into the development of this disease.

There are some pathological conditions for which blood vessels play an important role in their evolution. The most important case is the vascularization of malignant tumors. In order for the cancer cells to obtain appropriate nutrients to grow and to get rid of waste material, tumors need to be vascularized. Tumors achieve this by several methods such as cooption (use of pre-existing vessels) and angiogenesis [35]. Furthermore, most of the conditions induce changes in vessels at different levels. Cancer induces the development of abnormal, tortuous vessels [27], that can be reverted by successful treatment [40]. Images of the retina may provide information on pathological changes caused by local ocular diseases and early signs of certain systemic diseases [5, 109, 19, 104]. Other examples may be hypertension and diabetes, which induce the narrowing of the arteries. For example, a recent study has shown that retinal vessel microvascular structure is associated to risk of mortality from ischemic heart disease and stroke [104].

2.3 Image-based Diagnosis

Some comments on the imaging modalities are needed in order to understand their ability to image the vessels, their possible application in clinical tools and research studies, and the requirements that the Knowledge Representation Model (KRM) proposition needs to take into account. The diagnostic support provided by the vessel structure images is further made concrete by the specification of precise attribute measurements. These attributes will be the key elements of the KRM, so a justified introduction is mandatory.

2.3.1 Angiographic Modalities

Nowadays, there are many medical imaging modalities and protocols devised specifically for the visualization of vessels, that are generally denoted with the term *angiography*. Some of them include the injection of a modality-specific contrast agent that enhances the visualization of blood vessels[1].

Digital Substraction Angiography (DSA) is an evolution of the original *X-ray Angiography* (XA) technique, that digitally subtracts a pre-contrast image from a contrasted images obtained after injection of a contrast agent. Until recently, DSA has been considered the standard vessel imaging technique in many diagnostic and interventional procedures, such as assessment of renal and carotid artery stenosis, cerebral

[1] The first coronary *X-ray angiography* (XA) was performed accidentally by Sones and Shirey in 1958 [94]. While injecting contrast material in the right ventricle, the catheter slipped into the right coronary artery and for the first time discovered the advantages of imaging the vessels.

aneurysms, acute limb ischemia or arterio-venous malformations (AVMs) among others. The main advantage of DSA imaging is that it allows real-time, live visualization of very thin vessel structures, and thus can be used during interventional procedures. However, DSA involves radiation exposure, is a 2D modality and, more importantly, is an invasive procedure and thus, it has an associated risk of small complications. DSA is gradually being replaced by some non-invasive 3D imaging techniques, such as *Computerized Tomography Angiography* (CTA) and *Magnetic Resonance Angiography* (MRA).

CTA images are standard Computerized Tomography (CT) images generated by contrast injection simultaneously with the image acquisition. Depending on the synchronization of the image acquisition with the flood flow, different contrasts may be obtained, such as those corresponding to the arterial phase, venous phase, post-constrast phase, etc., that depict several stages of the contrast inflow into the vessels. Some of the applications of CTA imaging are analysis of stenosis in renal arteries, aortic aneurysms, brain aneurysms or AVMs, atherosclerosis assessment and detection of vein clots in legs. The main drawback of the technique is the radiation dose that the patient receives during the scanning procedure. With the advent of multidetector technology and improved computational image reconstruction schemes, acquisition haves increasing spatial resolution obtained in faster times with less radiation dose.

MRA comprises several techniques based on Magnetic Resonance Imaging (MRI). The techniques are based either on imaging flow effects or on using contrast agents, like in *Constrast-enhanced MRA* (CE-MRA). Vessel images can also be obtained by adequate pulse sequences without contrast. *Time-of-flight MRA* (ToF-MRA) uses a short echo time and flow compensation to enhance contrast of blood vessels. It is commonly used in the head and neck, where it gives very high resolution image, but has problems in areas of slow blood flow such as aneurysms. *Phase-contrast MRA* (PC-MRA) manipulates the phase of the MR signal providing both, the vessel image and the corresponding flow speed. PC-MRA has larger acquisition times, since the techniquerequires acquisitions in the three basic orientations (axial, sagittal and coronal). Recent MRI techniques include *Fresh Blood Imaging* (FBI) [66] and *Susceptibility Weighted Imaging* (SWI), also called *BOLD Venography* [83, 107]. The main advantage of MRA compared to CTA is the absence of radiation exposure while maintaining very high image quality, though spatial resolution is lower in MRA than in CTA. However, as acquisition times are larger, motion artifacts are more likely to appear.

Vessel Ultrasound imaging is a non-invasive procedure that allows live blood vessel visualization. Combined with the technique of Doppler ultrasound, it also gives measures of blood flow. It can help the physician to visualize and assess, stenoses, aneurysms, varicose veins and many other vessel accidents. The main problem is its low signal-to-noise ratio which gives poor image quality.

Optical imaging can also be used to image vessels, as in *Retinal Fundu*s images, where vessel analysis is used in the assessment of retinopathy and as an early sign of systemic diseases [5]. Other recent techniques, such such as non-invasive *Near-infrared* (NIR) imaging can be used for visualizing vessels through the skin [30].

Among the modalities that can provide vessel-related information other than the lumen, *Intravascular Ultrasound* (IVUS) provides a means of imaging the vessel wall by using a catheter equipped an ultrasound transducer. Another recent development is the study of the mechanic properties of vessel wall by *Magnetic Resonance Elastography* [105].

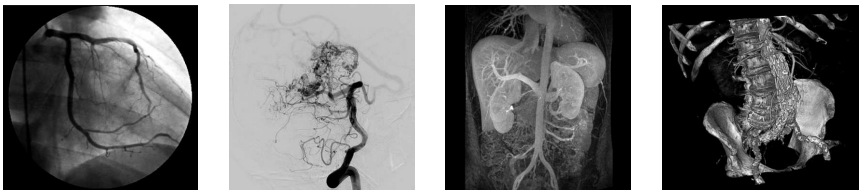

Fig. 1 Examples of Angiographic Modalities. From left to right XA of the coronaries, DSA of the brain vessels, MRA in venous phase and CTA showing stent after endovascular aortic aneurysm repair.

2.3.2 Applications of Vessel Analysis

As the technology of vessel imaging evolves, improving the quality and quantity of information about vessel structure that can be obtained, the applications have also flourished. Here we enumerate some of the current ones, that will motivate the knowledge representation and manipulation tools to be discussed below.

- Surgery
  - Surgery planning: allows the surgeon to evaluate the alternative actions and prepare for the intervention [89].
  - Planning and navigation [99] during interventional therapy and biopsy : here vessel structures are critical by themselves, but also serve as spatial reference or anatomical landmarks for planning and navigation. It has strong real-time requirements, because the vessel structure may be changing during the intervention. Sometimes it requires fusion of diverse imaging modalities to improve the interaction.
  - Training of surgeons and interventional radiologists using annotated virtual reality systems [98], virtual atlases, etc.
  - Follow-up after intervention to monitor the evolution of the affected tissues and areas [50].
- Cancer studies
  - Non-invasive estimation of tumor malignancy and growth by vessel quantification and localization of abnormal vessel clusters [15, 16].
  - Simulation and study of vessel angiogenesis, which is an important factor in malignant tumor growth [27].
- Diagnosis of vessel-related diseases by quantification of vessel attributes
  - Characterization of retinal-related diseases such as diabetic retinopathy or retinopathy of prematurity by induced changes in vessel attributes such as diameter and tortuosity [19].
  - Quantification of stenosis and aneurysms [41].
- Image registration using vessel as landmarks [63]. This is typically used in non-rigid registration [48].
- Studies of vessel morphometry [39] and haemodynamics [96]
  - Construction of geometric models of vessel trees [42] which allow direct visual diagnosis and fast and interactive visualization and exploration, and provide by themselves a good understanding of the (patient-specific) vessel network structure and morphology.

- Discovering of statistical properties of attributes of vessels in healthy and diseased populations [17].
- Performing comparative studies, possibly with the help of anatomical atlases, for assessment of vascular diseases, malformations and abnormalities.
- Simulation of arterial flow and pressure in organs that cannot be accessed by direct measurement [88], in aneurysms [101] or for detecting regions of turbulent flow prone to atherosclerosis, such as bifurcations and high-curvature regions [7].

2.3.3 Vessel Attributes

The main concern in this section is about measurements that can be somehow obtained from the images and used as a basis for diagnosis or any of the applications enumerated above. These measurements are the relevant attributes of the KRM proposed below for the feasible applications, therefore their identification from the literature survey is most important step in the KRM definition. Qualitative attributes are not integrated in any quantitative model, though they can result from computational image processing. They are used by the clinician to perform diagnoses or intervention decision upon their direct inspection. Structural attributes refer to the morphological and structural description of the vessel network. They are mostly used for intervention planning and some diagnoses based on structural morphology and complexity, like angiogenesis. The quantitative description of each vessel branch and bifurcation are the bricks of the decision support and model building processes.

Qualitative Vessel Attributes

- *Vessel Shape*: provided by direct visualization of volumes containing (contrasted) vessels, or surface reconstructions of the vessel walls.
- *Vessel Section Shape*: needs some processing and abstraction from the image in order to obtain an adequate representation. It may include the vessel wall or not, depending on the imaging modality.
- *Anatomical Location*:more important than the absolute anatomical position of the vessels is the relative position of the vessels with respect to adjacent organs or structures of interest, specially pathological structures. It may require some image registration techniques to obtain the corrected relative location.

Structural Vessel Attributes

- *Vessel Network Topology*: the topological structure and interconnections of the vascular network.
- *Total Number of Branches*: when restricted to a space, it is a measure of vessel density.
- *Depth Level*: this is the level of a branch with respect to the root branch of the vessel network, that is, the minimum number of bifurcations that separate the current branch from the root branch.
- *Strahler Number*: a numerical measure of branching complexity [95, 44].
- *Branching Frequency*: the number of bifurcations and distance between them.
- *Ratios of Branch Radii*: several measures can be obtained as ratios of branch radii in a bifurcation. The *branching ratio* and the *area expansion ratio* are related to the portion of flux going into each branch in a bifurcation [4].

Quantitative Vessel Attributes

- *Diameter*: is an immediate indicative of an aneurysm or stenosis.
- *Length*: though the absolute length of a branch may not be significative by itself, and its significance is relative, it can be used to calculate other important properties such as tortuosity.
- *Size/Volume*: volume and size of the vessels in a region of interest provides quantitative measurements of vessel growth.
- *Tortuosity*: is a property of a curve being twisted, having many turns. There have been several attempts to quantify this property [102]. Tortuosity is a sign of vessel abnormality usually associated to disease. Bullitt *et al.* [17] distinguish three types of blood vessels tortuosity:
  - *Type 1*: where vessels elongate and become tortuous. This may occur in conditions such as retinopathy, prematurity, hypertension and aging.
  - *Type 2*: vessels that make frequent changes of direction and may appear as a "bag of worms", as occurs in arteriovenous malformations and within hypervascular tumors.
  - *Type 3*: high-frequency low-amplitude oscillations or 'wiggles', associated to the neovascularity of malignant tumors.
- *Surface Area*: as arteries bifurcate and convert into arterioles and capillaries, the total surface area for the same blood supply increases.
- *Section Area*: this is the area of the vessel cross-sections, which lie in the normal plane to the medial line or centerline.
- *Blood Velocity*: differences in blood velocity can be measured or simulated in order to find stagnancy regions or abnormal circulation patterns.
- *Elasticity*: of the vascular walls that may change due to plaque accumulation or the presence of aneurysms.

2.4 Vessel Extraction and Analysis in Angiographic Images

The number of proposed algorithms for vessel detection and extraction from angiographic images is huge [52, 73, 45, 18, 26]. The approaches differ in the assumptions made about the shape and structure of the physical vessels, the medical imaging modalities, the mathematical models describing the vessels, the image features used to detect them, and the algorithmic schemes to extract them. In a recent outstanding review [52], vessel lumen segmentation techniques are categorized according to the underlying models (assumptions on appearance and geometry of the real vessels as shown in the images) image features (quantitative image metrics used to detect the vessels), and extraction schemes, (the algorithm used to extract the vessels, according to the assumed models and defined image features).

We proceed to describe the most important angiographic image-based vessel modelling and extraction (segmentation) techniques, emphasizing the most salient elements that are are explicitly modelled in our knowledge representation framework.

2.4.1 Vessel Models in Image-based Analysis

In image-based analysis of vascular networks, there are two main types of assumptions and models used for vessels: *photometric* models and *geometric* models. *Photometric*

models deal with the generation of vessel images in the corresponding angiographic modalities. They are modality dependent, used for image processing, and outside the scope of this paper. On the other hand, *geometric* vessel models describe elements such as branches, corresponding cross-sections, bifurcations and relationships in the vessel tree. They are relevant to the definition of our knowledge-based model which is more influenced by geometrical considerations.

Surface-only models of vessels, defined by polygonal meshes, which may be obtained directly from vessel segmentations by polygonal reconstruction [28], are not relevant to our endeavour because they are rather difficult to manipulate and useless as the basis for structural analysis and representation.

Vessels are elongated structures, except in some very specific (pathological) cases. For this reason, one of the most common approaches is to use the centerline as the main shape descriptor. The centerline corresponds to the medial loci of the vessel [10], centered inside the lumen, and constituting the centroid of successive cross-sections. The centerline allows to describe objects in terms of a tree of "elemental figures" [79]. However, it is very sensitive to vessel boundary details, so there has been an extensive research in algorithms that obtain smoother centerlines, such as Voronoi skeletons [69], shock loci of reaction-diffusion equations [91], "cores" (height ridges of medialness functions) [78] and distance transforms [12].

From the vessel's centerline, the external contour can be modelled as a generalized cylinder [3], that is, a tubular shape with a curvilinear axis (the centerline) and varying width along its length, which is usually defined by the cross-sections along the centerline. Different shape descriptors can be used to define these cross-sections (see figure 5). Constraints can be imposed on the successive sections in order to maintain spatial coherence when producing 3D models of vessels [70]. Sometimes the external surface of the vessel can be modelled explicitly [28] or implicitly [97] [7] from the vessel centerline. A mesh surface model of the vessel wall can also be obtained by sweeping the cross-sectional contours [47,68].

The tree structure of vessel networks is naturally described in the form of a graph, more specifically as trees (directed acyclic graphs) [32,14,89,2,76,64]. A vessel graph is obtained from the segmentation by skeletonization (see 2.4.2) and analysis of line structures. The graph description is useful for operations such as pruning, trimming, correcting and reconnecting of vessel branches via graph-based techniques after initial extraction. Graph-based representations can be mapped back into visual representations providing a better insight into the vascular structure by means of symbolic renderings [32] or surface reconstructions from centerline and section data [26].

2.4.2 Extraction Schemes

Because of its central importance, we dwell on the methods for centerline extraction found in the literature. Note that initial vessel volume segmentation can be obtained by techniques such as simple thresholding, region-growing [11], wave tracking [82] or vessel-adapted level-sets methods [55] among others.

*Centerline Extraction by Skeletonization*Centerlines can be extracted by 3D skeletonization of an initial volume vessel segmentation. Thinning algorithms [75] are based on iteratively removing points on the border of the object that do not modify its topology (simple points). The remaining set of points is the topological skeleton. The problem is that they usually provide a centerline at a pixel/voxel level. Subvoxel accuracy may

be obtained by other methods, such as flux of gradient vectors of distance functions [12].

Direct Centerline Extraction In some cases, a rough estimation of each slice's centerline point is enough to provide an approximate segmentation of the vessel tree, that may be useful for a more refined segmentation. This can be done by obtaining complete surfaces from the centerline, or on a section-by-section basis, by fitting models of sections or by extracting the section image planes and obtaining the boundaries by segmentation as in [49] (Figure 5).

The first approach to centerline extraction is interactive manual selection of centerline points and interpolation with or without an underlying mathematical curve model, such as a B-spline. However, this method is not very precise, and automatic algorithms are desiderable.

Direct centerline tracking algorithms start from a initial point or set of points, selected manually or automatically in the centerline or its vicinity, and try to iteratively extract consecutive vessel centerline points, usually by estimating vessel direction, until the end of the branch or tree is reached. Most of these methods also estimate the local vessel normal (section plane) and scale (approximate diameter) and differ mainly in the image features used for centerline tracking, in their ability to handle bifurcations and in their robustness to noise. We have found in the literature methods based on tracking multi-scale *medialness*[2] features [8], analysis of connected components of spheres [20], Kalman filtering [106], moments of inertia [33] and Bayesian tracking [51] among others.

Centerlines can also be obtained as *minimum cost paths* (geodesic paths) between start and end points detected on a branch or on the whole vessel tree. The inverse of the features or metrics used to estimate *medialness* measures can be used in this case as cost functions [103], minimized by optimization algorithms such as Dijkstra's shortest paths [24], graph-based schemes [72, 103], or the Fast Marching algorithm [1] used in [23].

Global Centerline Detection Centerlines can also be obtained by calculating vesselness or medialness features in the whole region of interest and by obtaining patches of centerlines by connected local maxima (ridges) of these features [80]. These patches are usually too wide and usually need to be skeletonized in order to obtain the medial representation that corresponds to the centerline. Other operations involve pruning, for removal of noisy branches, and reconnection of broken branches, as vessel features sometimes yield low values at bifurcations. For the reconnection, local strategies of the aforementioned minimum cost paths approaches can be used between candidate reconnection points.

2.4.3 Vascular Feature Models

Several vessel (disease-related) features can also be modelled. *Stenosis* are usually modelled as local diameter reductions [29, 53]. *Aneurysms* are more difficult to model and quantify due to their shape variability. Specific models have been proposed for cerebral [65] and aortic [58, 56] aneurysms. *Calcifications and stents* often appear as hyperintense structures. Recently, methods have been proposed that combine appearance and geometric models for the segmentation of these structures from CTA images [46,

[2] A medialness function quantifies to which degree a point is part of the centerline

100]. Recently, we proposed an automatic method for the detection of *endoleaks* after endovascular repair of aortic aneurysms [57].

2.5 Need for a Knowledge Representation Model

There are some examples of specialized vessel representation systems in the literature. The *Vascular Modelling Toolkit* [77] focuses on the geometric modelling of vascular structures in order to generate surface and mesh models suitable for structural and haemodynamic studies. Gerig *et al.* [32] proposed a symbolic model that encodes shape features and structure relationships of vessels obtained from segmentations of angiographic images, and applied it to the analysis of cerebral vasculature in MRA images. The hybrid model proposed by Puig *et al.* [81] provides information of the topological relationships of the vessels and incorporates vascular accidents such as aneurysms and stenoses as special vessel segments. It is organized in three layers: global structure, which is a graph-based structure, vascular surface and volume model. The model is constructed from segmented MRA images with application in a computer-assisted neurovascular system. The model proposed here tries to overcome some limitations of these early models, through a general yet flexible knowledge representation of vascular systems.

Common elements, components and stages found in our experience and literature review.

- In most of the cases, it is valid the assumption that the vessels are elongated, tube-like objects, whose length is much larger than the diameter.
- Vessels appear as hyperintense[3] structures (sometimes hypo) in the vascular imaging modalities, brighter that their neighboring tissues, though sometimes we can find contrast agent inhomogeneity or imaging artifacts.
- Homogeneity in vessel size and photometric intensity is desiderable, but usually it is necessary to deal with varying vessel widths and intensity inhomogeneities.
- The use of a vessel centerline, as a descriptor of the shape of the vessel and extraction and modelling of sections, is also a common element.
- Some schemes reuse well-known features, such as *medialness* functions. or intermediate representations, such as medial-based representations or skeletons.
- Some common processing stages can be identified in families of algorithms, for example, in vessel tracking procedures.

In fact, as emphasized in [52] many vessel algorithms rely on increasingly complex combinations of existing techniques, sometimes operating at different levels of abstraction. The identification of the building blocks that constitute the extraction schemes and the explicitation of some hidden assumptions and abstractions used in their conception is a crucial step for a better understanding of the underlying concepts for the improvement existing methods. This explicitation can be performed through the development of unified frameworks, which implement the most commonly used models, features and algorithms and identifying their appropriate settings.

In the present paper, we propose a unified framework focused on the modelling of vascular vessel networks and related qualitative and quantitative information. The framework models the vessel network in such a way that is easy to be handled by

[3] Hypointense vessel can be converted to hyperintense just by inverting the image intensities.

extracting schemes based on image analysis, but also to be converted into other representations suitable in several applications (see Figure 2). Such a framework will allow:

- an increased automation of the processes, which, in turn, increases the reproducibility of the experiments and allows to perform large quantitative studies which would be impossible to tackle otherwise.
- a quantitative comparison of the performance of different techniques under the same conditions and with known implementations, that may provide better insight into their behavior and that may lead to their optimization.
- an efficient reusability of components that will allow faster prototyping and more reproducibility in research studies.

Next, we will proceed to describe our *Vessel Knowledge Representation* (VKR) model in detail.

3 Requirements of the Vessel Knowledge Representation (VKR) Model

The VKR model is being defined through a process of identification and abstraction of structural, geometrical and morphological properties of vessels in the literature and in our own research experience. This leads to the identification of data structures, operations and components used in the most common models and schemes for vessel extraction. This model can then be converted into an appropriate data representation, such as a mesh surface model, a refined segmentation or a symbolic visual representation. When rendered, these representations can be used for localization and for interactive exploration of the VKR model and underlying properties in some of the applications described above. Alternatively, these derived data representations can also be used, for example, for numerical studies, such as simulations of haemodynamics, structural analysis or other medical and research applications out of the scope of this paper. The VKR model must include the geometry and topology of vessel trees with constituting branches, bifurcations and sections, as well as vascular accidents such as stenoses, aneurysms and abnormal regions, such as those feeding neighboring tumors. Models of these physical entities and related concepts used in vessel analysis applications must be devised and structured by using object-oriented design techniques.

We can make more precise some desired properties of our VKR model design:

- *Versatility*:
  - Modelling of low level entities, such as vessel centerlines or sections, without compromising higher level elements, such as the global graph-based model of the vessel tree and its traversal mechanisms.
  - Allowing several coexisting representations of the same vascular system, providing easy transformation among representations. This idea is illustrated in Figure 3 where different graph-based representation of the same vascular tree are shown.
  - Decoupling algorithms from underlying data structures. Abstract mechanisms must be provided for accessing, traversing and manipulating the data.
- *Efficiency*: as data amounts are huge in this kind of applications, and time requirements are increasingly tight, efficiency in terms of computational time and use of resources is highly desired.
- *Utility*: to be useful the VKR must take into account actual design practices and constraints from:

  - The vessel extraction algorithms (see 2.4.2) used for generating the vessel data structure from the angiographic image data.
  - A broad range of clinical and research applications that will be increasing in complexity and response time requirements.
- *Complexity Hierarchy*: the framework should be able to provide different levels of complexity and abstraction in order to represent the vessel structures at different levels. The structures need to be represented at least at the tree, branch and section level and at each level geometric, topological and semantic information layers need to be managed.
- *Integrability and Specificity*: the framework needs to be designed so it can be easily integrated into pre-existing frameworks which deal with certain specific models, processes and data structures efficiently, such as the *Insight Toolkit* [108], for medical image segmentation, registration and analysis and the *Visualization Toolkit* [87], for visualization of resulting vascular structures together with image data.

4 Model Description

4.1 The VKR Model in Context

The VKR model is the core of the diverse operations and functions related with vessel analysis techniques, as shown in the workflow diagram depicted in Figure 2. The boxes in this diagram correspond to data types of some kind, while the labeled arrows correspond to transformations or manipulations of the data. We have omitted the closed operations, such as branch pruning or image filtering. The VKR vessel representation can be obtained directly (see 2.4.2) from the angiographic image or volume or indirectly from the results of an intermediate image segmentation process. In the latter case, the segmentation detects the image/volume regions corresponding to the vessels, from which the vessel representation can be obtained by skeletonization (see 2.4.2), to obtain the centerlines, followed by section or boundary estimation. Alternatively, a set of disconnected volume vessel regions can be obtained by a global detection process of vessel features, followed by pruning and/or reconnection of centerline patches (see 2.4.2). We include in the diagram obvious storage and retrieval operation of the VKR to/from a file or database. The VKR model is the natural domain to perform measurements which can be added to it as an enrichment.

By assigning symbolic graphical representations or *glyphs* (such as lines, spheres, cones or more complicated shapes...) to the underlying components of the VKR model, a symbolic visual representation of the vessel tree can be obtained. This may be used as a roadmap, for agile exploration and interaction, or may be directly overlaid or projected onto the angiographic images, slices, or volumes in order to provide visual cues.

The VKR model can be the basis to build up a surface mesh of the vessel boundaries[4] by several techniques such as contour sweeping of the cross-sections or by an explicit or implicit surface model as explained in 2.4.1. The VKR model can also be used to generate a mask or ROI on the CTA/MRA volume for further processes. The VKR data can be then converted into a mesh surface by iso-surface reconstruction

[4] This is only feasible with volumetric angiographies, but the model is able to handle 2D representations too

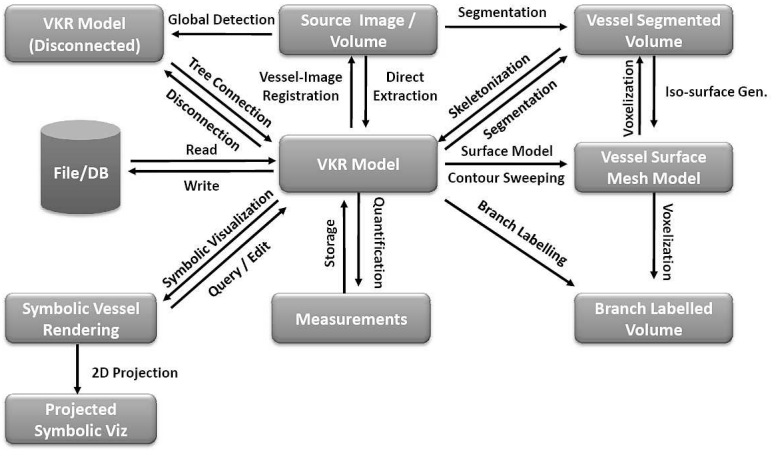

Fig. 2 VKR Workflow Diagram

[54]. Generated surface meshes can then be used for direct visualization and navigation, possibly mixed with other symbolic, surface, volume or slice renderings, in a kind of Augmented Reality computational environment. In the same spirit, the identified and labeled branches can be mapped into the CTA/MRA volume or mesh surface, allowing increased interaction via direct structure picking. The mapping can go both ways, allowing the access to the VKR model from the visualization of the CTA/MRA volume, and visualization of CTA/MRA data corresponding to VKR selections.

4.2 Data Structures

4.2.1 Vessel Graph

In general, we can consider the vessel network as a binary tree structure since in most cases bifurcations split a branch into two [39], with some exceptions like the Circle of Willis in the brain [88]. Therefore, a graph representation is the natural choice for the structural representation in the VKR.

A graph typically consists of nodes, representing the modelled concepts, and edges, that connect the nodes and represent their relationships, which is in terms of parent/child for tree structured graphs. In our case, a *VesselNode* represents an abstraction of an element used for vessel representation and analysis at graph level. Such an element may be a vessel branch, bifurcation or vessel accident, among others. Anatomical vessel branches are modelled as nodes[5] (*BranchNode*) and if we need to assign properties to the bifurcations, we can also explicitly model them (*BifurcationNode*). In order to provide more modelling flexibility, we define also *Composite* nodes, which make use of the *Composite Pattern* [31] in order to group nodes. This way the group of nodes acts as a single entity, hiding their internal relationships and offering the possibility of building a hierarchy of several levels of abstraction complexity in the graph.

[5] This differs from other works where nodes are modelled as graph edges [81]

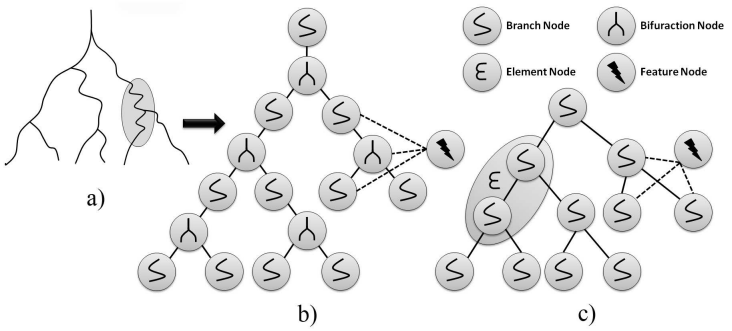

Fig. 3 Vessel Graph Representations. a) Symbolic depiction of a vessel tree b) BVG rep. c) BBVG Rep and OEVG after incorporating an *Element* supernode.

By inheritance of node objects we are also able to model conditions that occur in the branches themselves or in the surroundings (*FeatureNode*). We allow also nodes to model some abstract concepts, such as annotations that may be of interest in diagnostic applications. The properties of each node type are defined by specific attributes and operations and the use of OOP techniques such as polymorphism.

Our graph-based model, however, is not restricted to a tree structure, to provide the flexibility in its definition, that is necessary in some applications. For example, the number of parents of a node is not limited to one, although anatomical branches in general have a single parent. This flexibility allows for several types of representation of the same vessel network. The structure of these representations is open, since nodes can be, in principle, arranged in any desired manner. However, our model was designed at least to support a few representations that have been found useful for many vessel analysis applications. We will proceed to describe these representations and introduce the node types involved.

Branch Vessel Graph Representation The *Branch Vessel Graph Representation* (BVG) is the simplest representation of a vessel network in VKR. It consists of a graph of interconnected nodes of type *BranchNode*. This type of node is the most conspicuous in VKR models, since it represents the geometry and properties of vessel branches, which are the main constituents of physical vessel networks. The rest of the vessel network is in fact an abstraction of the relationship of vessel branches (such as bifurcations), related features, groupings of branches, etc. The most important part of a *BranchNode* is the *Centerline Model* that is described in section 4.2.3. Several *BranchNode* instances can be connected in series, in order to divide a branch into different segments. This might be useful to model parts of a branch which require special attention, such as stenotic or aneurysmal regions, and separate them from the healthy regions.

Branch-bifurcation Vessel Graph Representation The *Branch-bifurcation Vessel Graph Representation* (BBVG) explicitly models the bifurcations using a *BifurcationNode*. In this case, the parent and children of a *BifurcationNode* need to be a *BranchNode* or any subclass of it.

Ordered Element Vessel Graph Representation The *Ordered Element Vessel Graph Representation* (OEVG) is most suited for morphometric and haemodynamic stud-

ies, since serial branches of the same order, with the order defined according to the *Diameter-defined Strahler Ordering System* [44], are grouped into a *CompositeNode* called *ElementNode*. In an OEVG representation, *BranchNodes* that are not grouped can also be considered as *ElementNodes* since they also represent an element in Strahler's system. In haemodynamic circuits, a series of vessel branches of the same order are the equivalent to an electric circuit composed of resistances in series.

4.2.2 Vessel Branch

A virtual vessel branch is represented in VKR by a *BranchNode,* and it corresponds to the vessel segment that extends between consecutive bifurcations. A physical vessel branch may also be represented by several concatenated *BranchNode* instances. This would be useful when the user wants to make a difference between different parts along the length of a physical branch, for example by indicating that part of a branch is stenosed. This is performed by associating corresponding accident node representations, such as the *StenosisModel*, to the *BranchNode*. This will be better described in section 4.2.7. The core of a vessel branch in our model is represented by the *Centerline Model* described next.

4.2.3 Centerline Model

The vessel centerline or medial loci [10] is an important part of our model, since it is a good descriptor of elongated objects. Compared to other descriptors, such as boundary descriptors, the centerline captures better the vessel shape and provides a straightforward way of obtaining the relationships between the different branches of the vessel tree [92], since the centerline can be easily converted into a graph structure. Furthermore, it serves as a reference for calculating and storing local properties, both inside and on the boundaries of vessels. For example, the vessel length is measured along the centerlines and diameters are measured over sections whose center is the centerline. Therefore, we provide an explicit, yet flexible and agile, representation of the centerline.

The *Centerline Model* is designed to provide several degrees of increasing representation complexity, as shown in Figure 4 left. The simplest level of representation complexity is to define a centerline by its point descriptors, where a point descriptor is anything that may identify the location of a geometrical point on the centerline. Examples of point descriptors may be geometrical points in physical coordinates, image pixel indexes, chain-codes, etc. The next level of complexity involves defining the vessel normal section that defines the cross-sectional planes. On a third level, we can define a section model, thus allowing further levels of flexibility and complexity.

Our point-based *Centerline Model* is independent from the mathematical model used to define the centerline curve, whose points need to be defined explicitly in our model. The reason is that the centerline curve needs to be discretized in order to store local quantitative properties of the vessel centerline and sections, and to localize vessel accidents or other features of interest that need to be referred to some point on the curve. However, this does not preclude the definition of an interpolation mathematical model that can be assumed as a curve point generator. Examples of this could be a centerline curve defined as a B-spline by using control points. This can be implemented either by subclassing *Centerline* class or, as will be described in section 4.3.6, by decoupling the curve generation from its defining points, by providing an external generator by subclassing the *CenterlineAlgorithm* class.

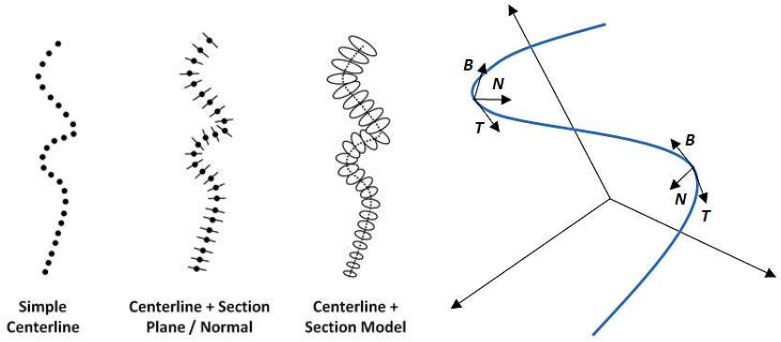

Fig. 4 Centerline Models (left) and Frenet reference frame for a 3D curve (right).

Finally, the *Centerline Model* provides a placeholder for optionally storing local centerline metrics which may provide valuable quantitative information about the local shape of the centerline. The most common and useful local centerline metrics, that can be defined at every point of the centerline, are the curvature, torsion (3D) and Frenet frame of reference, which includes the tangent, normal and binormal vectors (Figure 4 right). We contemplate an implementation (*LocalCurveMetrics* class) that generalizes this reference system to N-dimensions.

4.2.4 Section Model

Vessel Sections are localized at centerline points and they are assumed to vary along the vessel length. This variability is reflected in the parameters that define the section, for example, the diameter.

As we can see in Figure 5, vessel sections, like centerlines, can also be defined at increasing levels of complexity. The simplest level is to define the section as a circle, giving its center and radius/diameter. Since our sections are defined at explicit centerline points, the center is already given. The next level of complexity is an elliptical shape. More advanced mathematical models include radial functions and B-spline contours. The section can also be implicitly defined by a segmentation mask image or by level-sets of a higher dimensional function, that can be obtained by the level-sets method, based on evolution of implicit curves or surfaces [74]. Another possibility is that a section may define more than one contour. This is for example the case when we want to model the shape of the external and internal vessel wall or when we want to model the lumen and the aneurysm contour in abdominal aortic aneurysms). In the latter special case, the section is modelled in such a way that it can be shared by at least two different branches (*SharedVesselSection*) since a single aneurysm contour may extend to both iliac arteries.

These are just a few examples that demonstrate the versatility of the model. In this sense, our section model does not impose any shape model, the only condition is that it can be referred to centerline points.

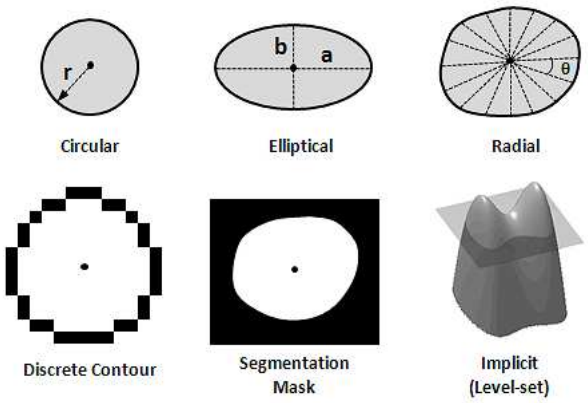

Fig. 5 Section Models

4.2.5 3D Surface and Voxel Models of Vessels

So far we have dealt with explicit modelling of cross-sections. Another possibility, when dealing with 3D image data, is to directly generate a 3D surface mesh from the centerline. If the 3D mesh is generated for the complete vessel tree, it can be referred to branches or even to centerline points (and thus to sections) of the VKR model by proximity to the corresponding centerline. This reference can be direct, by splitting the model into surface patches and keeping references to them, or indirect, simply by associating a scalar value, acting as identifier, to the mesh points that corresponds to referred branches. This way a forth-and-back relationship may be kept between the VKR and surface models. Explicit sections may also be obtained by intersection with corresponding section planes.

If a segmentation is available, obtained either *a priori* or from the VKR model, it can be referred to corresponding branches by just labelling the mask pixels/voxels with corresponding branch identifiers. In this case, keeping references to separate volume "patches" seems to be more difficult to handle but it is a possibility that could be useful in cases where the source angiographic volumes are huge. The reason is that, in most software frameworks, only arrays corresponding to rectilinear volumes can be stored, and for sparse structures such as the vessels, sometimes many of these voxels are empty. Another possibility is to store these labelled voxels as sparse images, which is currently not implemented.

4.2.6 Vessel Bifurcations

Bifurcations may be represented explicitly in the VKR model by means of the *BifurcationNode* object that defined at graph level. The use of this node type is optional (see BBVG representation in section 4.2.1), and may be required when we want to model special features of the bifurcation, when (quantification) operations need to be assigned to the bifurcation, such as estimation of branch angles, and when there may exist more than one parent branch.

4.2.7 Vessel Features

In the VKR model, vessel "features" (*FeatureNode*) represent special characteristics of the vessels that need to be highlighted. Their definition may include models for vessel accidents or simply comments used for diagnostic. A feature may affect or may be associated to a part of a branch, a whole branch or a set of branches, entirely or partially. In order to make explicit these relationships, two mechanisms are devised:

1. *FeaturesNodes* are assigned as children (or alternatively as parents) of affected *BranchNodes*. This is illustrated in Figure 3.
2. *FeatureNodes* keep a *VesselRegion* structure that indicates which vessel branches are affected and to which extent. This is achieved by keeping a set of *VesselBranch* node identifiers, and for each identifier, the starting and end indexes of the points in corresponding centerlines that comprise the area affected by the feature.

Since a feature may affect more than one branch, *FeatureNodes* are treated in a special manner and are not even visited when performing many operations that require traversal of the graph. In this sense, FeatureNodes can be treated as "hypernodes" and their relationship with *VesselBranch* nodes (or possibly other nodes) is not that of a parent-child relationship but merely a reference.

An example of use of a *FeatureNode* is to perform an annotation, such as a diagnostic remark in a application for computer aided vascular diagnosis. The clinician would choose the branches affected by a given feature, for example, those feeding a tumor or included on it, and assign them the corresponding nodes comment. Another possibility is to assign specific models of vessel accidents or disease, such as a *StenosisModel*, to a *FeatureNode* which are described next.

4.2.8 Models of Vessel Accidents or Disease

The VKR model offers the possibility of providing representation models for vessel accident or disease. Examples of these models are the *StenosisModel* and *AneurysmModel*. These models contain the quantitative morphological measurements and other properties that are typical of a given vessel accident or related disease. We provide flexibility for defining application-specific models of this kind.

There are two main possibilities for incorporating these models in the vessel graph: in a *BranchNode* or in a *FeatureNode*. The first option is more suitable for cases in which the accident affects a whole branch or a part of it. In this case, the affected area is modelled by a subclass of BranchNode (for example *StenosisBranchNode* or *AneurysmBranchNode*) that is connected serially in both extremes either to other *BranchNodes* or to *BifurcationNodes*. This configuration can be seen in Figure 7 and is further commented in section 4.3.6. Another possibility is incorporating the model into a *FeatureNode* as explained in the previous section. This is more appropriate in cases in which the accident affects more than one branch.

4.3 Supported Operations

Operations that can be performed on the VKR model data structures can be classified by their nature or by the type of object they operate on. For example, quantification operations can be performed at graph, branch, centerline or section level, among others. Based on their nature we distinguish the following types:

- *Access Operations*: these are abstract access mechanisms that allows to perform other types of operations. For example, graph traversal is an operation that allows to access nodes on the vessel graph and perform other operations on them.
- *Edition Operations*: allows to change the internal structure and properties of the model.
- *Quantification Operations*: evaluation of quantitative measurements over different elements of the model.
- *Input/Output Operations*: used to load and save the model data.
- *Data Transformation Operations*: include generation of the VKR model and transformation into another representation that can be useful for intended applications.
- *Model-specific Operations*: these are internal operations that are specific to certain elements of the model, such as the centerlines or sections.

4.3.1 Access Operations

Graph Traversal The most important access operation is graph traversal. Graph traversal operations can be performed efficiently by using the *Visitor Pattern [31]* object-oriented technique (*GraphVisitor*). This pattern allows to decouple the structure of the graph and corresponding nodes from the operations performed of them. This is desirable because it constitutes and efficient manner of extending the framework with new operations. The visitor abstracts the mechanism of traversing the graph according to a set of rules that are defined by the user. For example the user may choose to visit only some specific type of nodes, such as bifurcations or may use node masks to enable/disable visiting specific nodes. Subclasses define specific traversal rules and the operation to be performed. Operations at any depth level that need to be performed on the whole vessel tree are implemented this way.

Model Picking Picking operations are those that allow to access structures of the VKR model by selecting them from a derived representation, either symbolic or geometric. They constitute the random access means to any part of the VKR.

Picking operations are based on established relationships between the target structures of the model (nodes, branches or sections) and their representation. This can be performed directly, by keeping references (pointers) to the structures on the model, or by assigning corresponding identifiers as explained in subsection 4.2.5 for surface meshes and volumes. Another possibility to establish this relationship is by proximity in terms of Euclidean distance. For example, a user could pick a point on the surface and the closest centerline point or section could be selected and its properties displayed.

4.3.2 Model Editing Operations

Most edition operations can be implemented in a straightforward manner by exposing the internal structure of the data after a picking operation. Of particular interest are graph editing operations, which alter the structure of the graph by changing the relationships between nodes and insert or delete nodes on demand. Graph editing operations can be performed interactively by the user, i.e. to correct artifacts in VKR models produced during its extraction, or by autonomous algorithms, i.e. deleting noisy branches based on their absolute length or underlying image values.

4.3.3 Quantification Operations

Quantification operations can be performed once the initial graph structure of the vessels has been created. Some of these quantitative measures are calculated and stored in the model on-the-fly, when they are part of the necessary calculations performed by the vessel extraction algorithms. Some other quantification operations are only performed on demand, on the whole vessel tree or on a part of it, since they may be computationally expensive. Whole tree calculations are performed via specific graph visitors. These visitors may incorporate other specific objects to perform quantification at deeper levels. For example, a *CenterlineMetricsCalculatorVisitor* object traverses the tree searching for centerlines of *BranchNodes*. At each centerline, a *CenterlineMetricsCalculator* object calculates local centerline metrics. If we want to calculate metrics for a single centerline, we can access it directly and use this latter object instead of using the visitor object.

Quantification can be performed at almost every level in the VKR model. A reference diagram of some of the attributes that can be measured is shown in Figure 6. The diagram shows the data model on which the operations are performed and the locality and type of measurement (i.e. geometrical, topological, image-based...) in a hierarchical manner. Some of the measurements are directly stored in the corresponding data structures or placeholders of the VKR model. Others can be obtained from the object that performs the operations.

4.3.4 Input/Output Operations

Input/Output (I/O) operations are intended to store/recover instances of the VKR model data structures. Two main types of I/O operations are initially considered: file and database I/O operations. The chosen format for file operations has been *GraphML* [13]. It is an XML-based format specifically designed for serializing graph information and that can be extended for custom needs. It allows to explicitly define the graph nodes, its relationships as edges[6]. Attributes can also be assigned to nodes and edges, allowing to store properties. On the other hand, application-specific relational databases can be designed, mimicking the data structures of the VKR model.

4.3.5 Data Transformation Operations

Data transformation operations involve conversions between high-order vessel representations and are summarized in the VKR workflow diagram in Figure 2. Except for graph-to-graph operations, they consist of generation of the VKR model from external image data and transformations to other types of data representations used in corresponding applications. Many of these external operations are not yet implemented, but for the sake of completeness, we describe some of these operations and important considerations here.

Graph-to-graph Operations These operations convert a vessel graph into another vessel graph in which the configuration of the nodes has changed. This is possible because the nature and openness of the graph representation in the VKR model allows the definition of different types of graphs and nodes, and thus, conversion operations between graph

[6] In our model, graph edges are implicitly defined as references or pointer to nodes

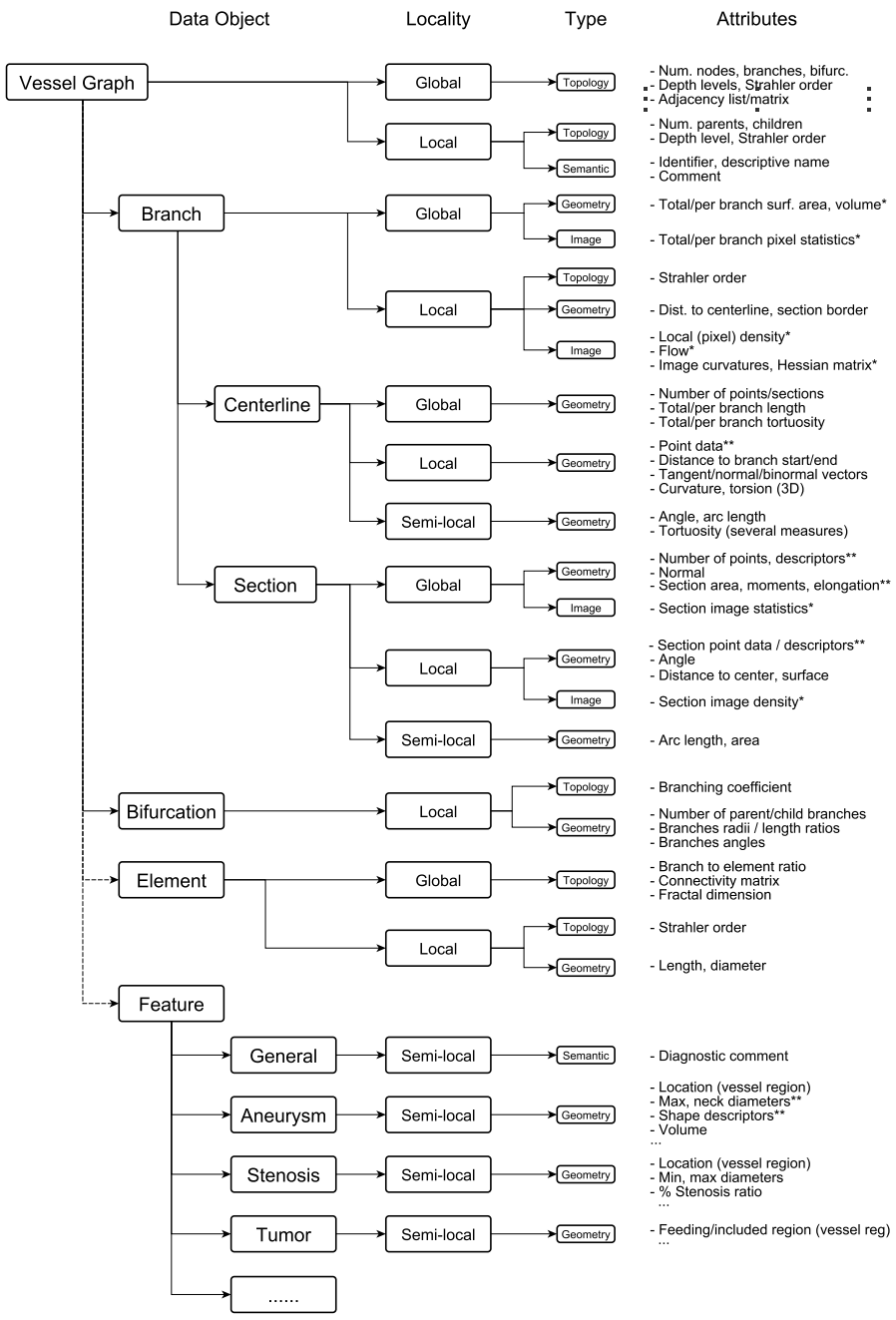

* Properties that require a reference to external data source (image, surface mesh, velocity field) to be calculated
** Definition of these measures is very open and not imposed by the model

Fig. 6 Quantitative attributes

types. We do not include here operations that transform inner data structures only, such as the centerlines. Typical graph operations are conversions between vessel graphs representation described in section 4.2.1.

Another operation of this type is converting a disconnected set of branches obtained by global detection algorithms into a vessel graph (see Figure 2). This is the equivalent of having a container of disconnected nodes which are organized into a complete graph by establishing the links.

Image-to-graph Operations These correspond to the VKR model construction from the image/volume by using vessel extraction schemes as the ones described in section 2.4.2.Some schemes may use intermediate representations, such as a segmentation mask or a disconnected set of nodes (see Figure 2).

Graph-to-image Operations Sometimes it is necessary to convert the graph into a voxel representation (segmentation) that also involves branch labelling. This can be used, for example, for overlaying and blending this labelled segmentation on top of the original image and assigning a color to each label. These labels can also be used as region of interests, to limit further processing operations on the source image to corresponding branches.

Another set of graph to image operations is projection on 2D images (see Figure 2). A typical example is when we have a VKR model obtained from a 3D angiography (such as CTA or MRA) and we want to project part of the model, such as the centerline on a 2D X-ray angiography, in order to visualize the real paths of some vessels that may be occluded.

Graph-to-mesh Operations These operations convert a vessel graph into a surface mesh. The conversion depends on the actual representation of the graph. It can be obtained by contour sweeping or by using a predefined mesh model either explicitly or implicitly as described in section 2.4.1 among other techniques.

4.3.6 Model-specific Operations

We describe some model-specific operations that are not included in the previous classes of operations and that are exclusive of the corresponding representations.

Graph Operations We consider here operations that modify the attributes of common nodes only, because graph operations will be specified in terms of node operations and visitor patterns.

Graph Labelling is a straightforward operation that assigns unique labels to nodes. *Node Wrapping/Unwrapping* are operations that transform a vessel graph into another vessel graph in which some nodes are wrapped into a supernode (subclass of *CompositeNode*) and viceversa. Node wrapping may require specific rules by which nodes are merged into a single supernode. On the other hand, node unwrapping may work without setting any rules by simply restoring the underlying nodes. A specific wrapping operation is defined in order to convert a (B)BVG rep. into a OEVG rep. (see section 4.2.1) as defined in [39].

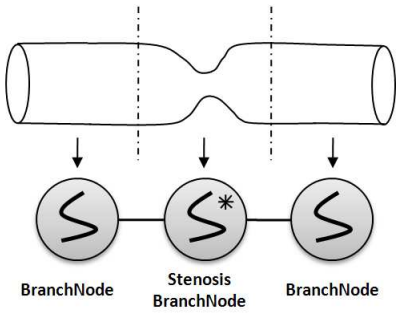

Fig. 7 Example of branch splitting operation to indicate an stenosis. A single *BranchNode* is split into three serial nodes, where the middle node incorporates a *StenosisModel*.

Branch Operations Operations that affect the branches as a whole are included here. A specific operation for branches is assigning them an *order* in the (modified) Strahler ordering system (see section 2.1). This involves traversing all branches from the leaves to the roots. If the diameter-defined method is used, this requires iteratively assigning orders and calculating diameters.

Branch splitting is the operation of dividing a branch into several branches. This operation (see Figure 7) may be performed, for example, to mark a region of a branch as having a specific accident or disease model. *Branch merging* is the contrary operation, where several branch patches are merged into a single branch node. They can be also considered as edition operations (see section 4.3.2).

Section interpolation is an operation that needs to be considered at branch level, since it involves both, generation of new intermediate centerline points, that define the section location, and estimation of section normal and boundary according to the corresponding model.

Centerline Operations Centerline operations involve modification of the points that define a centerline. Centerline generation operations, such as centerline tracking or skeletonization (see section 2.4.2and 2.4.2), lie in this group, but they are usually part of the vessel extraction schemes that explicitly deal with centerlines and are not considered here.

Centerline interpolation is the process of resampling an existing centerline, or one that is being created, following a given mathematical model of curve. For example, if the distance between centerline points is not uniform, a linear resampling may produce uniform sampling. Another possibility is to fit the centerline curve to a set of connected B-spline curves.

Centerline filtering may also be used to convert a rough, noisy centerline into a smoother centerline, by removal of points or by several types of smoothing filters, such as average, median or anisotropic diffusion filters that operate on centerline points.

Centerline registration is the process of converting a centerline into another centerline by applying a rigid or elastic transform to the points of the centerline. This transform is obtained by minimization of a cost function, that is usually based on image-values. Examples of centerline registration applications are comparison of vessel geometrical features between different patients [84] or quantification of aneurysms and stenosis [41].

Section Operations Section operations involve generally modification of the geometry of the section, or reestimation of the section normal[7]. As in the previous case, these operations can be performed after or during the vessel extraction procedure. In the second case, section generation can be considered as an inherent part of the extraction schemes described in 2.4.2 but, like in the case of the centerline, some of the algorithms can be applied at a post-processing stage.

Section interpolation can be performed in two ways, either by interpolating the section geometry according to its mathematical representation (resampling of points, etc.) or by interpolating sections by creating new intermediate sections. In the later case, it also involves a modification of the centerline and as such, can be considered a branch operation (see section 4.3.6).

Section filtering involves geometric filtering of noisy boundaries. It is similar to centerline filtering and depends greatly on the section model.

5 Implementation Details

In Figure 8 an UML diagram of the most important objects in the VKR model is depicted. We do not pretend to be exhaustive, but only to give an accurate overview of the main object definitions and their relationships. According to their function, we can distinguish two main types of objects: data representation objects (left), that describe the vascular structure, and algorithmic objects (right), that implement operations on the data representation objects. As can be seen, there is almost a one-to-one correspondence between data objects and algorithms. This separation between data objects and algorithmic objects provides more flexibility, since it makes easy to define new algorithms without affecting the data representations. Other more straightforward operations are implemented as methods of the corresponding data objects. In Figure 8 we have set a horizontal line that separates the depth level of the objects: data structures and algorithms above this line correspond to graph level whereas those below the line operate at underlying modelling levels.

The highest level data structure is the *VesselGraph* which may contain one or several root nodes. All vessel graph nodes are subclasses of the *GraphNode* abstract class, which provides generic node-handling operations and metadata such as node identifiers, and *VesselNode* which is an abstract class specific for nodes of vessel graphs. We chose not to model explicitly the edges of the graph. Thus, the graph consists of nodes, that are connected by virtual links, which are implemented as references (pointers) to the corresponding nodes. *GraphNodes* contain a set of children nodes, as strong references, and a set of parent nodes, as weak references [8].

Due to their importance, we provide a brief description of some salient implemented node types:

– *BranchNode*: is the most important node type, which represents the physical vessel segment that extends between two bifurcations. A *BranchNode* contains a *Centerline*. We decided to implement the centerline as a placeholder of *Section* objects, where the simplest section model is a point that represents the centerline, instead of keeping a list of points on the centerline model itself. This forces a one-to-one

[7] reestimation of the section center corresponds to a centerline operation

[8] Strong references imply a composition relationship and weak references an aggregation

mapping and provides the flexibility for a non-explicit centerline definition. Centerline points are thus the centers of *Section* objects, and can be defined with any descriptor that identifies their geometrical position, such as euclidan coordinates, image indexes, chain-codes, etc.. The same applies for the points that define the section boundaries. This provides much flexibility in defining the centerline and section for a wide range of applications. In general, this type of flexibility is provided in the VKR model by using *Generic Programming* techniques [25].

- *BifurcationNodes* are more simple in their definition. They explicitly reference confluent branches as parent/child nodes and their use is optional (see Figure 3). Algorithms may be devised to operate on bifurcation nodes to take advantage of the direct access to confluent branches.
- *CompositeNodes* are nodes obtained by wrapping other nodes and exposing the internal links only. The information about internal nodes and links is kept when wrapping is performed, so the situation can be reversed easily. This ability may provide several types of simultaneous representations of the vessel graph, as can be seen in Figure 3 (right). One direct application is converting the branch nodes of the same (modified) Strahler order into a single element using the node type *ElementNode*.
- *FeatureNodes* indicate relevant features in vessels and incorporate an optional feature model that describes the corresponding feature such as an stenosis (*StenosisModel*) or aneurysm (*AneurysmModel*). They incorporate a *VesselRegion* structure that indicates the area affected by the feature in corresponding branches.

With respect to the algorithms, those that operate at graph level are subclasses of *GraphNodeVisitor* and *VesselGraphNodeVisitor*. The use of the *Visitor Pattern* [31], allows to separate the node definition from the operations on the graph by decoupling the graph traversal from the node operations. These graph-level algorithms can be classified according to the objects they ultimately operate on. An algorithm may operate at graph level because only graph elements are involved in the corresponding algorithms. An example is calculating the number of nodes in the branch, or computing the (modified) Strahler order of *BranchNodes*. Another possibility is that they encapsulate algorithms that operate at deeper levels (such as the level of centerline or section) but are applied to the corresponding structures on the whole graph and not only locally. In this sense, the level of encapsulation of the data structure finds a correspondence in the level of encapsulation of the algorithms. This makes possible to reuse local algorithms and apply them to the whole graph. An example is the family of *CenterlineAlgorithm* classes, which perform operations on a single centerline. These operations can be performed for all the centerlines of the *BranchNodes* of a vessel graph by defining a specific visitor (*CenterlineAlgorithmVisitor*) which encapsulates the former.

In Figure 9 we can see a representation of the external operations (we call them "filters" here) that can be performed in order to create the VKR Model and to convert it to other (3D) representations, such as surface meshes or segmentation masks. Objects of type correspond to the vessel extraction schemes commented in section 2.4.2. Such an extraction scheme, may use the VKR Model as an intermediate representation and then use an algorithms of type *VesselGraphToImageFilter* to obtain the final segmentation or a *VesselGraphToSurfaceFilter* object to obtain a surface mesh.

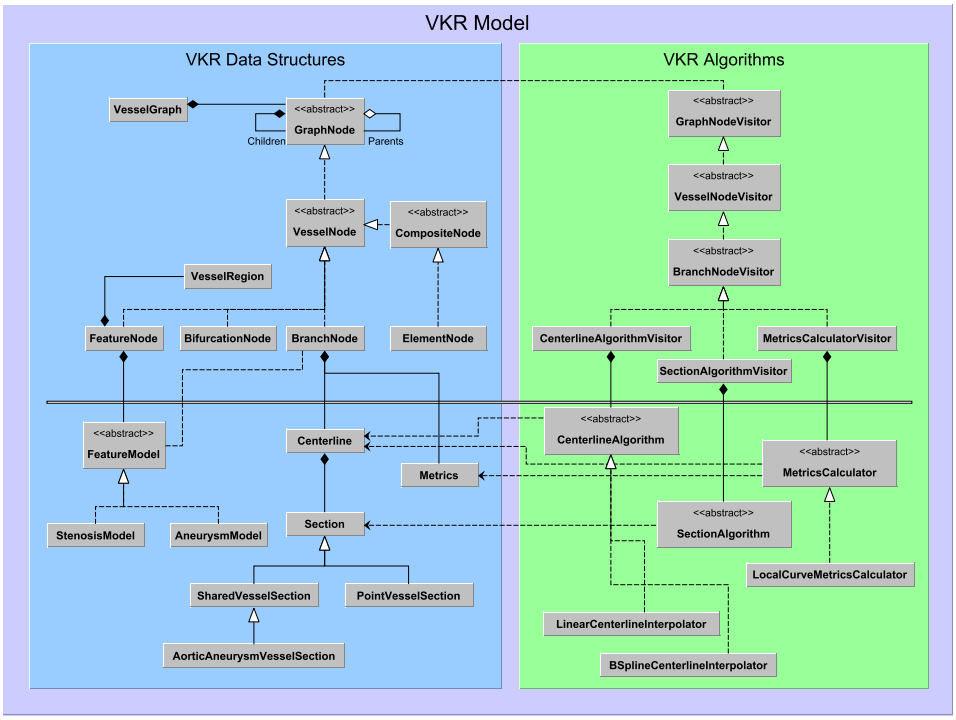

Fig. 8 VKR Model. Internal Implementation

Finally, most high-level objects, such as filters, nodes, centerlines or sections are implemented using reference counting, so they can be shared by many objects without unnecessary copies and additional overhead.

Needless to say, implementation is an on-going never-ending process, as long as applications, imaging resources and computational algorithms evolve. Therefore, the description given of current state and trends of our implementation must be assumed as a core implementation aiming at a continuing incremental process incorporating new algorithms, accepting new imaging resources and addressing innovative applications.

6 Conclusions

The evergrowing applications and techniques of Blood Vessel Analysis have produced a complex landscape of algorithms and data representations that hinders the composition of procedures, the reuse of software and the comparative analysis in terms of computational efficiency and quality of final results (visualization, measurement, edition, and others). We have detected the need of proposing a foundational Vessel Knowledge Representation (VKR) model that may allow the exchange of data among applications and users. One of the goals of VKR is the reuse of software pieces, providing a ground functional layer that may serve as the basis for new developments, thus alleviating development efforts. The model can be used as an intermediate representation between image-based extraction schemes and clinical and research applications,

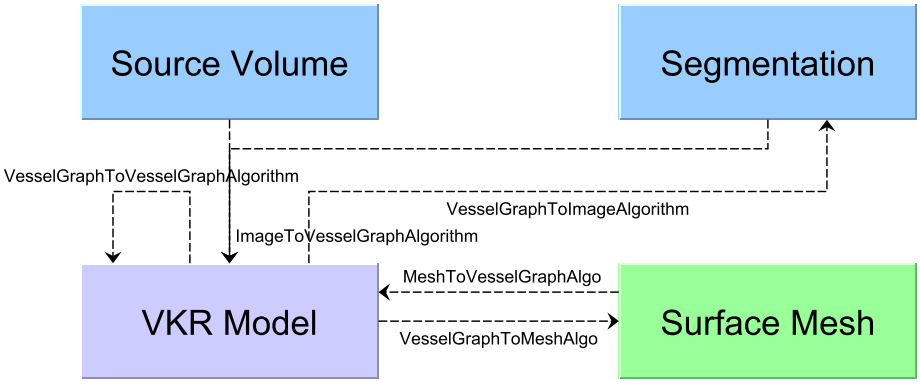

Fig. 9 VKR Model. External Implementation

to perform quantitative measurements on extracted vessel structures and to provide the necessary vessel representation and handling tools for the target applications. In this paper we have identified, from the literature and our own research work, the key knowledge representation items, as well as the key operations that are the building blocks for nowadays and future vessel analysis processes and applications.

VKR provides a versatile and efficient object-oriented representation of vessel structures and associated algorithms and quantitative data. It contemplates flexible data representations for the vascular tree, underlying structures such as branches, bifurcations, centerlines and sections, as well as vessel features such as stenosis, aneurysms, etc. It also contemplates operations and algorithms that operate efficiently on corresponding data structures. Furthermore, the model is designed so it can be easily integrated with pre-existing frameworks. We are already applying the VKR model in vessel-related applications related to our current research areas.

References

1. D. Adalsteinsson and J. A. Sethian. A fast level set method for propagating interfaces. *J. Comput. Phys.*, 118(2):269–277, 1995.
2. G. Agam, S. G. Armato III, and C. Wu. Vessel tree reconstruction in thoracic ct scans with application to nodule detection. *IEEE Trans. Med. Imaging*, 24:486–499, 2005.
3. G. J. Agin and T. O. Binford. Computer description of curved objects. *IEEE Trans. on Computers*, 25(4):439–449, Apr 1976.
4. S. Aharinejad, W. Schreiner, and F. Neumann. Morphometry of human coronary arterial trees. *The Anatomical Record*, 251:50–59, 1998.
5. K. Akitaa and H. Kugaa. A computer method of understanding ocular fundus images. *Pattern Recognition*, 15(6):431–443, 1982.
6. L. Antiga, B. Ene-Iordache, and A. Remuzzi. Computational geometry for patient-specific reconstruction and meshing of blood vessels from mr and ct angiography. *Medical Imaging, IEEE Transactions on*, 22(5):674 –684, May 2003.
7. L. Antiga and D. A. Steinman. Robust and objective decomposition and mapping of bifurcating vessels. *Medical Imaging, IEEE Transactions on*, 23(6):704 –713, june 2004.
8. S. R. Aylward and E. Bullitt. Initialization, noise, singularities, and scale in height ridge traversal for tubular object centerline extraction. *IEEE Trans. Med. Imaging*, 21(2):61–75, February 2002.
9. L. Bezold. Coronary artery anomalies, Jan 2010.

10. H. Blum. A transformation for extracting new descriptors of shape. In Weiant Wathen-Dunn, editor, *Models for the Perception of Speech and Visual Form*, pages 362–380. MIT Press, 1967.
11. T. Boskamp, D. Rinck, F. Link, B. Knmmerlen, G. Stamm, and P. Mildenberger. New vessel analysis tool for morphometric quantification and visualization of vessels in ct and mr imaging datasets. *Radiographics*, 24:287–297, 2004.
12. S. Bouix, K. Siddiqi, and A. Tannenbaum. Flux driven automatic centerline extraction. *Medical Image Analysis*, 9(3):209–221, June 2005.
13. U. Brandes, M. Eiglsperger, I. Herman, M. Himsolt, and M. S. Marshall. Graphml progress report: Structural layer proposal. In *Graph drawing. International symposium No9, Vienna, LNCS*, volume 2265, pages 501–512, 2002.
14. E. Bullitt, S. Aylward, K. Smith, S. Mukherji, M. Jiroutek, and K. Muller. Symbolic description of intracerebral vessels segmented from magnetic resonance angiograms and evaluation by comparison with x-ray angiograms. *Medical Image Analysis*, 5:157–169, 2001.
15. E. Bullitt, G. Gerig, S. Aylward, S. Joshi, K. Smith, M. Ewend, and W. Lin. Vascular attributes and malignant brain tumors. In *Medical Image Computing and Computer-Assisted Intervention (MICCAI 2003), LNCS*, volume 2878, pages 671–9. Springer, 2003.
16. E. Bullitt, I. Jung, K. Muller, G. Gerig, S. Aylward, S. Joshi, K. Smith, W. Lin, and M. Ewend. Determining malignancy of brain tumors by analysis of vessel shape. In *Medical Image Computing and Computer-Assisted Intervention (MICCAI 2004), LNCS*, volume 3217, pages 645–653, 2004.
17. E. Bullitt, K.E. Muller, I. Jung, W. Lin, and S. Aylward. Analyzing attributes of vessel populations. *Medical Image Analysis*, 9:39–49, 2005.
18. K. Bühler, P. Felkel, and A. La Cruz. Geometric methods for vessel visualization and quantification - a survey. In *Geometric Modelling for Scientific Visualization*, pages 399–420. Springer-Verlag, 2002.
19. Ali Can, Hong Shen, James N. Turner, Howard L. Tanenbaum, and Badrinath Roysam. Rapid automated tracing and feature extraction from retinal fundus images using direct exploratory algorithms. *IEEE Trans. Inform. Technol. Biomed*, 3:125–138, 1999.
20. J.F. Carrillo, M. Hernández-Hoyos, E.E. Dávila-Serrano, and M. Orkisz. Recursive tracking of vascular tree axes in 3d medical images. *Int. J. of Computer Assisted Radiology and Surgery*, 1(6):331–9, 2007.
21. M. A. Creager, T. F. Lüscher, F. Cosentino, and J. A. Beckman. Diabetes and vascular disease: Pathophysiology, clinical consequences, and medical therapy: Part i. *Circulation*, 108:1527–32, 2003.
22. G. Cumming, L. K. Harding, K. Horsfield, K. Prowse, S. S. Singhal, and M. J. Woldenberg. Morphological aspects of the pulmonary circulation and of the airway. *Fluid Dynamics of Blood Circulation and Respiratory Flow*, 65:230–6, 1970.
23. T. Deschamps and L. Cohen. Deschamps, t., cohen, l., 2001. fast extraction of minimal paths in 3d images and applications to virtual endoscopy. med. image anal. 5 (4), 281-299. *Medical Image Analysis*, 5(4):281–299, 2001.
24. E. W. Dijkstra. A note on two problems in connection with graphs. *Numerische Mathematik*, pages 269–271.
25. G. Dos-Reis and J. Järvi. What is generic programming? In *Proc. of the First International Workshop of Library-Centric Software Design (LCSD'05)*, Oct 2005.
26. P. Felkel, A. Kanitsar, A. L. Fuhrmann, and R. Wegenkittl. Surface models of tube trees. In *In Computer Graphics International*, pages 70–77, 2002.
27. J. Folkman. Incipient angiogenesis. *J. Natl. Cancer Inst.*, 92:94–5, 2000.
28. A. Frangi, W. Niessen, R. Hoogeveen, T. van Walsum, and M. Viergever. Model-based quantitation of 3-d magnetic resonance angiographic images. *IEEE Trans. Medical Imaging*, 18(10):946–956, 1999.
29. A. Frangi, W. J. Niessen, P. J. Nederkoorn, O. van Elgersma, and M. A. Viergever. Three-dimensional model-based stenosis quantification of the carotid arteries from contrast-enhanced mr angiography. In *IEEE Workshop on Mathematical Methods in Biomedical Image Analysis*, 2000.
30. I. Fridolin and L. G. Lindberg. Optical non-invasive technique for vessel imaging: I. experimental results. *Phys. Med. Biol.*, 45(12):3765–78, 2000.
31. E. Gamma, R. Helm, R. Johnson, and J. Vlissides. *Design Patterns: Elements of Reusable Object-Oriented Software*. Addison-Wesley, 2000.

32. G. Gerig, T. Koller, G. Székely, C. Brechbuhler, and O. Kubler. Symbolic description of 3d structures applied to cerebral vessel tree obtained from mr angiography volume data. In *Information Processing in Medical Imaging '93, LNCS 687*, pages 94–111, 1993.
33. M. Hernández-Hoyos, P. Orlowski, E. Piatkowska-Janko, P. Bogorodzki, and M. Orkisz. Vascular centerline extraction in 3d mr angiograms for phase contrast mri blood flow measurement. *Int. J. Computer Assisted Radiology and Surgery*, 1(1):51–61, March 2006.
34. M. Heron, D. L. Hoyert, S. L. Murphy, J. Xu, K. D. Kochanek, and B. Tejada-Vera. Deaths: Final data for 2006. Report, Division of Vital Statistics, U.S. Dep. of Health and Human Services, 2009.
35. J. Holash, P. C. Maisonpierre, D. Compton, P. Boland, C. R. Alexander, D. Zagzag, G. D. Yancopoulos, and S. J. Wiegand. Vessel cooption, regression and growth in tumors mediated by angiopoietins and vegf. *Science*, 284(5422):1994–8, 1999.
36. K. Horsfield. Morphometry of the small pulmonary arteries in man. *Circulation Research*, 42:593–7, 1978.
37. K. Horsfield. Diameters, generations, and orders of branches in the bronchial tree. *Journal of Applied Physiology*, 68:457–461, 1990.
38. K. Horsfield and I. Gorden. Morphometry of pulmonary veins in man. *Lung*, 159:211–8, 1981.
39. W. Huang, R. T. Yen, M. McLaurine, and G. Bledsoe. Morphometry of the human pulmonary vasculature. *Journal of Applied Physiology*, 81:2123–33, 1996.
40. R. K. Jain. Normalizing tumor vasculature with anti-angiogenic therapy: a new paradigm for combination therapy. *Nature Med.*, 7:987–998, 2001.
41. D. G. Kang, D. C. Suh, and J. B. Ra. Three-dimensional blood vessel quantification via centerline deformation. *IEEE Trans. Medical Imaging*, 28(3):405–414, March 2009.
42. K. L. Karau, G. S. Krenz, and C. A. Dawson. Branching exponent heterogeneity and wall shear stress distribution in vascular trees. *AJP Heart and Circulatory Physiology*, 280:1256–63, 2001.
43. G. S. Kassab. Scaling laws of vascular trees: of form and function. *AJP Heart and Circulatory Physiology*, 290:894–903, 2006.
44. G. S. Kassab, C. A. Rider, N. J. Tang, and Y. C. Fung. Morphometry of pig coronary arterial trees. *Am. J. Physiol.*, 265:350–365, 1993.
45. C. Kirbas and F. Quek. A review of vessel extraction techniques and algorithms. *ACM Computing Surveys*, 36(2):81–121, June 2004.
46. A. Klein, W. K. J. Renema, L. J. Oostveen, L. J. Schultze Kool, and C. H. Slump. A segmentation method for stentgrafts in the abdominal aorta from ecg-gated cta data. In X. P. Hu; A. V. Clough, editor, *Proc. SPIE Medical Imaging 2008: Physiology, Function, and Structure from Medical Images*, volume 6916, 2008.
47. R. Klein, A. Schilling, and W. Strasser. Reconstruction and simplification of surfaces from contours. In *Proc. 7th Pacific Conf. on Comp. Graphics and App.*, 1999.
48. T. Lange, S. Eulenstein, M. Huumlnerbein, and P. M. Schlag. Vessel-based non-rigid registration of mr/ct and 3d ultrasound for navigation in liver surgery. *Computer Assisted Surgery*, 8(5):228–240, 2003.
49. J. Lee, P. Beighley, E. Ritman, and N. Smith. Automatic segmentation of 3d micro-ct coronary vascular images. *Medical Image Analysis*, 11(6):630–647, 2007.
50. J. H. Legarreta, F. Boto, I. Macía, J. Maiora, G. García, C. Paloc, M. Graña, and M. de Blas. Hybrid decision support system for endovascular aortic aneurism repair follow-up. In *Proc. of 5th Int. Conf. on Hybrid Artificial Intelligent Systems (HAIS'10)*, page Submitted, 2010.
51. D. Lesage, E. Angelini, I. Bloch, and G. Funka-Lea. Medial-based bayesian tracking for vascular segmentation: Application to coronary arteries in 3d ct angiography. In *IEEE Int. Symp. Biomed. Imaging (ISBI'08)*, pages 268–271, 2008.
52. D. Lesage, E.D. Angelini, I. Bloch, and G. Funka-Lea. A review of 3d vessel lumen segmentation techniques: Models, features and extraction schemes. *Medical Image Analysis*, 13(6):819–845, December 2009.
53. Q. Lin. *Enhancement, Extraction and Visualization of 3D Volume Data*. PhD thesis, Institute of Technology, Linköpings Universitet, 2003.
54. W. E. Lorensen and H. E. Cline. Marching cubes: A high resolution 3d surface construction algorithm. *Computer Graphics, Vol. 21, Nr. 4, July 1987*, 21(4):163–9, 1987.
55. L.M. Lorigo, O. Faugeras, W.E.L. Grimson, R. Keriven, R. Kikinis, and C.F. Westin. Co-dimension 2 geodesic active contours for mra segmentation. In *IPMI*, pages 126–139, 1999.

56. M M. de Bruijne, B. van Ginneken, W. J. Niessen, M. Loog, and M. Viergever. Model-based segmentation of abdominal aortic aneurysms in cta images. In *Proc. SPIE Med. Imaging*, volume 5032, pages 1560–71, 2003.
57. I. Macía, M. Graña, C. Paloc, and F. Boto. Neural network-based detection of type ii endoleaks in cta images after endovascular repair. *Int. J. of Neural Systems*, page Submitted, 2010.
58. I. Macía, J. H. Legarreta, C. Paloc, M. Graña, J. Maiora, G. García, and M. de Blas. Segmentation of abdominal aortic aneurysms in ct images using a radial model approach. In E. Corchado; H. Yin, editor, *Proc. Intelligent Data Engineering and Automated Learning, 10th Int. Conference (IDEAL'09)*, volume 5788 of *Lecture Notes in Computer Science (LNCS)*, pages 664–671, Burgos, Spain, Sep 2009. Springer.
59. I. Macía, D. Wald, and C. Paloc. Extraction and analysis of patient-specific hepatic anatomy from mr images. In *Int. J. of Computer Assisted Radiology and Surgery. Proc. of the 22st Int. Congress and Exhibition (CARS'08)*, volume Suppl. 1, pages 399–401, Barcelona, Spain, Jun 2008.
60. J. Maiora, G. García, I. Macía, J. H. Legarreta, F. Boto, C. Paloc, M. Graña, and J. Sánchez. Thrombus volume change visualization after endovascular abdominal aortic aneurysm repair. In *Proc. of 5th Int. Conf. on Hybrid Artificial Intelligent Systems (HAIS'10)*, page Submitted, 2010.
61. J. Maiora, G. García, I. Macía, J. H. Legarreta, C. Paloc, M de Blas, and M. Graña. Thrombus change detection after endovascular abdominal aortic aneurysm repair. In *Proc. of Computer Assisted Radiology and Surgery (CARS'10)*, page In press, 2010.
62. J. Maiora, G. García, A. Tapia, I. Macía, J. H. Legarreta, C. Paloc, M. Graña, and M. de Blas. Stent graft change detection after endovascular abdominal aortic aneurysm repair. In E. Corchado; H. Yin, editor, *Intelligent Data Engineering and Automated Learning - IDEAL 2009 10th Internationa Conference, Proceedings*, volume 5788 of *Lecture Notes in Computer Science (LNCS)*, page 826, Universidad de Burgos, Burgos, Spain, Sep 2009. Springer.
63. J. H. Metzena, T. Krögerb, A. Schenk, S. Zidowitz, H. O. Peitgen, and X. Jiang. Matching of anatomical tree structures for registration of medical images. *Image and Vision Computing*, 27(7):923–933, Jun 2009.
64. J. Mille and L. D. Cohen. Deformable tree models for 2d and 3d branching structures extraction. In *IEEE Conf. on Computer Vision and Pattern Recognition Workshops*, 2009.
65. R. D. Millán, L. Dempere-Marco, J. M. Pozo, J. R. Cebral, and A. F. Frangi. Morphological characterization of intracranial aneurysms using 3-d moment invariants. *IEEE Trans Med Imaging*, 26(9):1270–82, 2007.
66. M. Miyazaki, N. Ichinose, S. Sugiura, H. Kanazawa, Y. Machida, and Y. Kassai. A novel mr angiography technique: Speed acquisition using half-fourier rare. *Journal of Magnetic Resonance Imaging*, 8(2):505–7, 2005.
67. C. Murray. The physiological principle of minimum work, i: the vascular system and the cost of blood volume. *Proc. Natl. Acad. Sci. USA*, 12(3):207–214, 1926.
68. O. Nilsson, D. Breen, and K. Museth. Surface reconstruction via contour metamorphosis: An eulerian approach with lagrangian particle tracking. In *In Proc. 16th IEEE Visualization (VIS'05)*, 2005.
69. M. Näf. *3D Voronoi Skeletons: a Semicontinuous Implementation of the 'Symmetric Axis Transform' in 3D Space*. PhD thesis, ETH Zürich, 1996.
70. T. O'Donnell, T. Boult, X. Fang, and A. Gupta. The extruded generalized cylinder: A deformable model for object recovery. In *Proc. of Computer Vision and Pattern Recognition (CVPR'94)*, pages 174–181, 1994.
71. S. Oka and M. Nakai. Optimality principle in vascular bifurcation. *Biorheology*, 24(6):737–751, 1987.
72. S. Olabarriaga, M. Breeuwer, and W. J. Niessen. Minimum cost path algorithm for coronary artery central axis tracking in ct images. In *Med. Image Computing and Computer Assisted Intervention (MICCAI'03)*, 2003.
73. M. Orkisz, L. Flórez-Valencia, and M. Hernández-Hoyos. Models, algorithms and applications in vascular image segmentation. *Machine Graphics and Vision*, 17(1/2):5–33, 2008.
74. S. Osher and J. A. Sethian. Fronts propagating with curvature-dependent speed: Algorithms based on hamilton-jacobi formulations. *J. Comput. Phys.*, 79:12–49, 1988.

75. K. Palágyi, E. Sorantin, E. Balogh, A. Kuba, C. Halmai, B. Erdohelyi, and K. Hausegger. A sequential 3d thinning algorithm and its medical applications. In *Proc. of the 17th Int. Conf. on Information Processing in Medical Imaging (IPMI'01), LNCS*, volume 2082, pages 409–415. Springer Verlag, 2001.
76. M. Paradowski, H. Kwasnicka, and K. Borysewicz. Capillary blood vessel tortuosity measurement using graph analysis. In *Knowledge-Based and Intelligent Information and Engineering Systems, 13th Int. Conf. (KES 2009)*, 2009.
77. M. Piccinelli, A. Veneziani, D. A. Steinman, A. Remuzzi, and L. Antiga. A framework for geometric analysis of vascular structures: Application to cerebral aneurysms. *Transactions on Medical Imaging*, 28(8):1141 –55, Aug 2009.
78. S. M. Pizer, D. Eberly, B. S. Morse, and D. S. Fritsch. Zoom-invariant figural shape: The mathematics of cores. *Computer Vision and Image Understanding*, 69:55–71, 1998.
79. S. M. Pizer, K. Siddiqi, G. Székely, J. N. Damon, and S. W. Zucker. Multi-scale medial loci and their properties. *International Journal of Computer Vision*, 55(2-3):155–179, 2003.
80. T. Pock, C. Janko, R. Beichel, and H. Bischof. Multiscale medialness for robust segmentation of 3d tubular structures. In *10th Computer Vision Winter Workshop*, 2005.
81. A. Puig, D. Tost, and I. Navazo. Hybrid model for vascular tree structures. In Liere R. van Leeuw, W. de, editor, *Data Visualization 2000 : Joint Eurographics and IEEE TCVG Symposium on Visualization, Amsterdam, The Netherlands*, pages 125–135. Springer-Verlag, 2000.
82. F.K.H. Quek and C. Kirbas. Vessel extraction in medical images by wave-propagation and traceback. *IEEE Trans. Med. Imaging*, 20(2):117–131, February 2001.
83. J. R. Reichenbach, R. Venkatesan, D. J. Schillinger, D. K. Kido, and E. M. Haacke. Small vessels in the human brain: Mr venography with deoxyhemoglobin as an intrinsic contrast agent. *Radiology*, 204:272–7, 1997.
84. L. M. Sangalli and S. Vantini. Registration of functional data: Aligning inner carotid artery centerlines. In *Proceedings of the XLIV Riunione Scientifica Società Italiana di Statistica*, 2008.
85. W. P. Santamore and A. A. Bove. Why arteries are the size they are. *Journal of Applied Physiology*, 104:1259, 2008.
86. M. Schaap, C.T. Metz, T. van Walsum, A.G. van der Giessen, A.C. Weustink, N.R. Mollet, C. Bauer, H. Bogunovic, C. Castro, X. Deng, E. Dikici, T. O'Donnell, M. Frenay, O. Friman, M. Hernández Hoyos, P.H. Kitslaar, K. Krissian, C. Kühnel, M.A. Luengo-Oroz, M. Orkisz, Ö. Smedby, M. Styner, A. Szymczak, H. Tek, C. Wang, S.K. Warfield, Y. Zhang, S. Zambal, G.P. Krestin, and W.J. Niessen. Standardized evaluation methodology and reference database for evaluating coronary artery centerline extraction algorithms. *Medical Image Analysis*, 13(5):701–714, 2009.
87. W. Schroeder, K. Martin, and B. Lorensen. *The Visualization Toolkit: An Object-Oriented Approach to 3D Graphics*. Kitware, 4th edition edition, 2006.
88. M. Schwarz, M. P. Nguyen, U. Kiencke, C. Heilmann, R. Klemm, C. Benk, F. Beyersdorf, and H. J. Busch. Integration of the circle of willis into avolio's model of the arterial hemodynamics. In *6th IASTED Int. Conf. on Biomedical Engineering*, 2008.
89. D. Selle, B. Preim, A. Schenk, and H. O. Peitgen. Analysis of vasculature for liver surgical planning. *IEEE Trans. Med. Imaging*, 21:1344–57, 2002.
90. T. F. Sherman. On connecting large vessels to small: the meaning of murray's law. *Journal of General Physiology*, 78:431–453, 1981.
91. K. Siddiqi and B. B. Kimia. A shock grammar for recognition. cvpr'96:507-513, san francisco, ca, ieee. In *IEEE Computer Vision and Pattern Recognition (CVPR'96)*, pages 507–13, 1996.
92. K. Siddiqi and S. Pizer. *Medial Representations: Mathematics, Algorithms and Applications*. Springer, 2008. ISBN 978-1402086571.
93. S. Singhal, R. Henderson, K. Horsfield, K. Harding, and G. Cumming. Morphometry of the human pulmonary arterial tree. *Circulation Research*, 33:190–7, 1973.
94. F. M. Sones and E. K. Shirey. Cine coronary arteriography. *Modern Concepts of Cardiovascular Disease*, 31:735–8, 1962.
95. A. N. Strahler. Hypsometric (area-altitude) analysis of erosional topology. *Geological Society of America Bulletin*, 63(11):1117–42, 1952.
96. R. Torii, M. Oshima, T. Kobayashi, K. Takagi, and T. E. Tezduyar. Influence of wall elasticity in patient-specific hemodynamic simulations. *Computers & Fluids*, 36(1):160–8, 2007.

97. C. van Bemmel, O. Wink, B. Verdonck, M. Viergever, and W. Niessen. Blood pool contrast-enhanced mra: Improved arterial visualization in the steady state. *IEEE Trans. Medical Imaging*, 22(5):645–652, 2003.
98. I. van Herzeele, R. Aggarwal, and I. Malik. Use of simulators in vascular training. *Heart*, 95:613–4, 2009.
99. P. M. A. van Ooijen, G. de Jonge, and M. Oudkerk. Coronary fly-through or virtual angioscopy using dual-source mdct data. *Eur Radiol.*, 17(11):2852–59, Nov 2007.
100. D. Vukadinovic, T. van Walsum, R. Manniesing, S. Rozie, R. Hameeteman, T. T. de Weert, A. van der Lugt, and W. J. Niessen. Segmentation of the outer vessel wall of the common carotid artery in cta. *IEEE Transactions on*, 29(1):65–76, Jan. 2010.
101. S. Wang, J. Chen, X. Yang, and X. Zhang. Patient-specific hemodynamic analysis for cerebral aneurysm. In *Proc. Bioinformatics and Biomedical Engineering (ICBBE'08), 2nd Int. Conf. on*, 2008.
102. C. M. Wilson, K. D. Cocker, M. J. Moseley, C. Paterson, S. T. Clay, W. E. Schulenburg, M. D. Mills, A. L. Ells, K. H. Parker, G. E. Quinn, A. R. Fielder, and J. Ng. Computerized analysis of retinal vessel width and tortuosity in premature infants. *Investigative Ophthalmology and Visual Science*, 49(8):3577–3585, 2008.
103. O. Wink, W.J. Niessen, and M.A. Viergever. Multiscale vessel tracking. *IEEE Trans. Med. Imaging*, 23(1):130–133, 2004.
104. N. Witt, T. Y. Wong, A. D. Hughes, N. Chaturvedi, B. E. Klein, R. Evans, M. McNamara, S. A. M. Thom, and R. Klein. Abnormalities of retinal microvascular structure and risk of mortality from ischemic heart disease and stroke. *Hypertension*, 47:975–981, 2006.
105. D. A. Woodrum, A. J. Romano, A. Lerman, U. H. Pandya, D. Brash, P. J. Rossman, L. O. Lerman, and R. L. Ehman. Vascular wall elasticity measurement by magnetic resonance imaging. *Magnetic Resonance in Medicine*, 56:593–600, 2006.
106. S. Worz and K. Rohr. Segmentation and quantification of human vessels using a 3-d cylindrical intensity model. *IEEE Trans. on Image Processing*, 16(8):1994–2004, 2007.
107. Q. Yang, J. Liu, S. R. S. Barnes, Z. Wu, K. Li, J. Neelavalli, J. Hu, and E. M. Haacke. Imaging the vessel wall in major peripheral arteries using susceptibility-weighted imaging. *Journal of Magnetic Resonance Imaging*, 30(2):357–365, 2009.
108. T. S. Yoo, M. J. Ackerman, W. E. Lorensen, W. Schroeder, V. Chalana, S. Aylward, D. Metaxas, and R. Whitaker. Engineering and algorithm design for an image processing api: a technical report on itk - the insight toolkit. *Stud. Health. Technol. Inform.*, 85:586–592, 2002.
109. L. Zhou, M. S. Rzeszotarski, L. J. Singerman, and J. M. Chokreff. The detection and quantification of retinopathy using digital angiogram. *IEEE Trans. Med. Imaging*, 13:619–626, 1994.
110. Y. Zhou, G. S. Kassab, and S. Molloi. On the design of the coronary arterial tree: a generalization of murray's law. *Phys. Med. Biol.*, 44:2929–45, 1999.